Physical Modelling in Geotechnics

The influence of saturation on the dynamic response of the structure behind a retaining wall

X. Guan & G.S.P. Madabhushi
Schofield Centre, Engineering Department, University of Cambridge, UK

ABSTRACT: Excavation near buildings for new infrastructure is sometimes unavoidable due to increasing congestion in urban areas. During earthquakes, the foundations of buildings adjacent to a retaining wall may suffer significant damage due to the excessive soil deformation around them as the retaining wall deforms. However, the interaction between the retaining wall and the buildings has not been well understood. To investigate the structural response of the buildings next to retaining walls, two dynamic centrifuge tests were conducted on two retaining walls with the same structure placed on the backfill in dry and saturated sand respectively. The accelerations of the structure and retaining walls are presented. Additionally, the rotations of the structure and the bending moments in the retaining walls are shown. It shows that the soil condition (i.e. dry or saturated) influences the dynamic behaviour of the structure and the retaining wall differently.

Keywords: structure, retaining wall, earthquake, saturation, structural movement.

1 INTRODUCTION

In the construction of new structures, such as buildings, bridges, and coastal structures, especially near existing structures, retaining walls are commonly built to ensure the safety of structures. However, such retaining wall systems including the adjacent structures can be vulnerable in seismic zones. During an earthquake, the retaining walls and the soil behind can experience large deformation and movement, resulting in uneven settlements under the foundations of the adjacent buildings. The difference in the foundation settlements can lead to damage or even collapse of the buildings.

The failure mechanisms of retaining walls have been widely studied. However, the research on the dynamic behaviour of the structures near the retaining walls is rather limited. Since such a topic has yet been thoroughly understood, studies using physical modelling may be performed, laying a foundation for further research and numerical validation.

2 EXPERIMENTAL METHODOLOGY

Centrifuge modelling was employed in this research. The scaling laws that were introduced by Schofield (1980) and Madabhushi (2017) link a small-scaled model to its realistic prototype. Two dynamic centrifuge tests were conducted in the Turner Beam centrifuge at the Schofield Centre. The centrifuge has a radius of 4.125m and has a capacity of 150g-ton.

2.1 Structural design

Two cantilever retaining walls are made of aluminium with the same thickness of 3mm. The height of the retaining wall in the dry test is 156mm, while the height of the retaining wall in the saturated test is 260mm. The details of the two model walls are summarised in Table 1. These dimensions and the flexural stiffness for the two walls are shown in the prototype scale.

The structure behind the retaining wall is a portal sway frame structure with a height of 243mm. Its prototype is a mid-rise building with two separate strip foundations. The natural frequency of this structure is 1.2Hz in the prototype scale, which is within the frequency range of many past earthquakes. The main body of the structure is made of aluminium. A block that is made of brass at the top of the slab of the structure is to create a difference in the bearing pressure of the strip footings. The bearing pressure under the left and right footings are 83kPa and 117kPa respectively.

Table 1. Properties of the retaining walls in the dry and saturated tests (prototype scale).

Wall no.	Height (m)	Thickness (m)	Flexural stiffness (MNm^2/m)
Wall 1	9.36	0.18	34.02
Wall 2	15.6	0.18	34.02

2.1 Model preparation

Both centrifuge models were tested in a container with rigid boundaries. This container has an inner dimension of 730mm × 250mm × 398mm (length × width × height). To minimise the reflection of the p-wave in the models, some Duxseal was placed next to the side walls (Steedman and Madabhushi, 1991). The front side of the container is made of transparent Perspex allowing for image analysis.

The models in both dry and saturated tests were prepared with Hostun sand utilising the automatic sand pouring machine at the Schofield Centre (Madabhushi et al., 2006). The moving speed of the nozzle from which the sand pluviated was constant to achieve satisfactory uniformity. The parameters, including the dropping height, spacing and nozzle size, in the sand pouring were calibrated for the target relative density of 40% (loose sand). The characteristics of Hostun NH 31 sand are summarised in Table 2.

Table 2. Properties of Hostun NH31 sand (Mitrani, 2006).

Property	Value
Maximum void ratio (e_{max})	1.01
Minimum void ratio (e_{min})	0.555
Specific gravity (G_s)	2.65

For the saturated test, the sand was saturated with an aqueous solution of hydroxypropyl methyl cellulose with a viscosity of ~60 cSt. The model was flushed with carbon dioxide that is heavier than air and is soluble in water to achieve a high degree of saturation. Before saturation started, both models in the container and the fluid in the holding tank were under vacuum pressure. The fluid flowed to the model container when a difference in the vacuum pressure was created. The flow rate of the fluid, ~1kg/h in this model, was controlled by the pressure difference.

The layouts of the centrifuge models are shown in Fig.1. The same embedment ratio, i.e. the ratio of the retained height over the embedment depth, was applied to both dry and saturated tests, which was 0.625.

2.3 Instrumentation and facilities

Microelectromechanical system accelerometers (MEMS) were used to measure the horizontal and vertical accelerations at different locations of the portal sway frame structure and the retaining walls. Strain gauges were installed in the retaining wall to measure the bending moments. The locations of these accelerometers and strain gauges are shown in Fig.1.

A high-speed and -resolution camera was used for particle image velocimetry (PIV) analysis. The camera was fixed to a gantry facing the transparent side of the container. During the test, images were taken at a high rate of ~900 frames per second. Markers were glued to the footings and the retaining wall for tracking their movements.

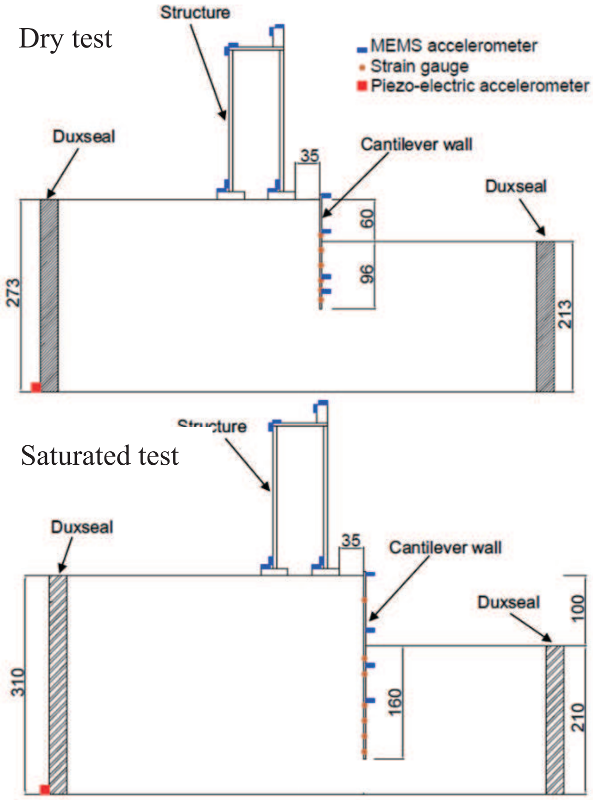

Fig. 1. Centrifuge models in dry and saturated tests (in mm).

2.4 Input earthquake loading

The input accelerations were generated with a servo-hydraulic earthquake actuator (Madabhushi et al., 2012). Six earthquakes were fired on the dry sand model, while only four earthquakes were fired due to the collapse of the structure behind the retaining wall during the fourth earthquake. The characteristics of the input earthquake loading are summarised in Table 3.

Table 3. Details of the fired earthquakes in two tests (prototype scale).

No.	Dry test			Saturated test		
	Type	Peak acc. (g)	Freq. (Hz)	Type	Peak acc. (g)	Freq. (Hz)
EQ1	Sinusoidal	0.10	1	Sine sweep	0.05	-
EQ2	Scaled Kobe	0.18	-	Sinusoidal	0.09	1
EQ3	Sine sweep	0.03	-	Scaled Kobe	0.09	-
EQ4	Sinusoidal	0.24	1	Sinusoidal	0.27	1
EQ5	Sinusoidal	0.15	1.2	-		
EQ6	Sinusoidal	0.33	1	-		

3 RESULTS

To investigate the dynamic behaviour of structures from a more realistic perspective, this paper focuses on the results obtained when the models were subjected to the scaled Kobe earthquake.

3.1 Dynamic behaviour of the structure

Figs. 2 and 3 show the horizontal accelerations of the structure in the dry and saturated tests, respectively. The accelerations are normalised by the average peak accelerations of the input motions in the positive and negative directions. The results from fast Fourier transform analysis and response spectrum analysis are also presented. In both dry and saturated tests, the proportion of the low-frequency components increased when the shear waves were transmitted to the top of the structure. Additionally, the frequency components in the accelerations of the structure base are similar to those of the input accelerations, but with an amplification in the magnitudes. Such an increase is due to the amplified accelerations occurring when shear waves were transmitted in dry or saturated sand from the bedrock to the surface. However, in the dry test, a significant peak at the frequency of ~1 Hz was observed in the FFT plots of the accelerations at the top of the structure. This frequency component is slightly smaller than the measured natural frequency of the structure with a fully fixed base, as expected.

Some differences lie in the dynamic response spectra. Specifically, at the top of the structure placed on dry sand, a peak spectral acceleration was observed at the frequency of around 1 Hz (1s), which did not occur in the saturated test. The spectral accelerations at the top of the structure were smaller than those of the input accelerations in the saturated test in the frequency range from 1.3 Hz (0.75 s) to 1.7 Hz (0.6 s). However, in the dry case, the spectral accelerations within this range were slightly more than those obtained from the input motions.

Fig. 4 shows the rotation of the structure during earthquake loading in the dry and saturated tests. Despite the fired earthquakes had larger amplitudes in the dry test, the structure rotated only 0.1º, which was much less than the residual rotation of 0.6º in the saturated tests. Additionally, less oscillation was witnessed in the structural rotation in saturated sand. Instead, twice significant rotation occurred, resulting in sudden increases in the permanent rotational movement. In contrast, the structure placed on the dry backfill moved back and forth during the earthquake, before which a moderate increase had occurred in the permanent rotation of the structure when the amplitudes of the input earthquake were relatively larger in the beginning.

3.2 Dynamic behaviour of retaining walls

The time histories and FFT plots of the accelerations at different elevations of the retaining walls are shown in Fig. 5 and Fig. 6. The magnitudes of the accelerations at the wall tip were noticeably larger than those at the rest of the wall in both dry and saturated tests, as the wall tip was free from the restriction of the sand. Furthermore, the amplification at the wall tip was more significant in the dry test than in the saturated test.

Fig. 7 shows the normalised bending moments in the retaining walls before, during and after the earthquake. The peak dynamic bending moments were larger than residual bending moments in both dry and saturated tests. However, the peak bending moments approximately doubled in the dry test, compared to those in the saturated test. Additionally, the peak bending moments of the wall in the dry test were higher than those in the saturated test.

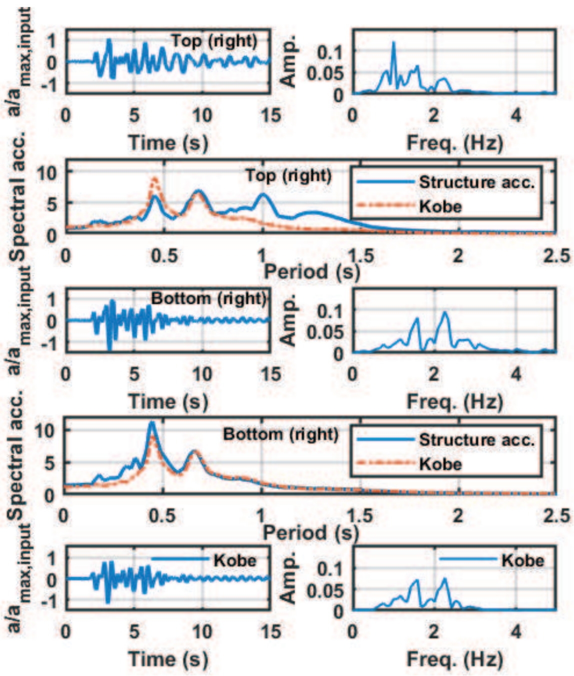

Fig. 2. Dynamic response of the portal sway frame structure in the dry test.

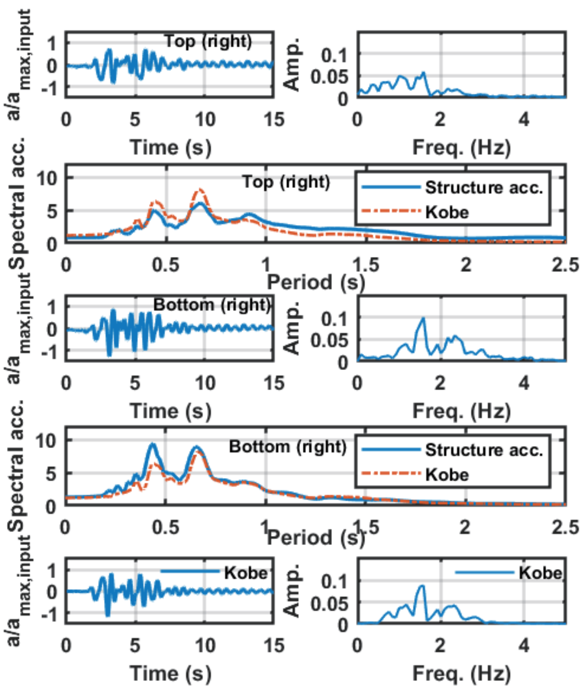

Fig. 3. Dynamic response of the portal sway frame structure in the saturated test.

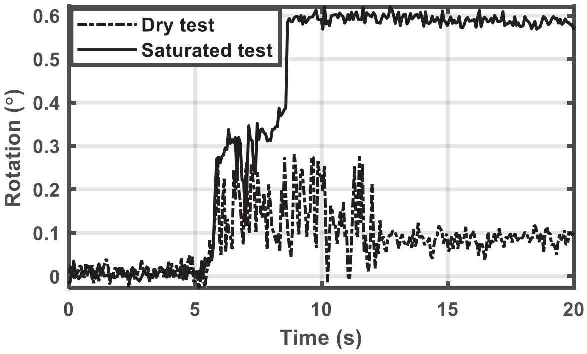

Fig. 4. Rotation of the portal sway frame structure in the dry and saturated tests.

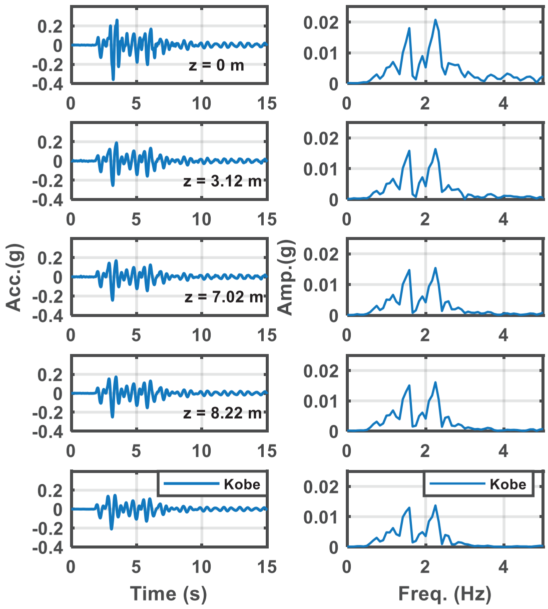

Fig. 5. Acceleration time histories at various elevations of the retaining wall in the dry test.

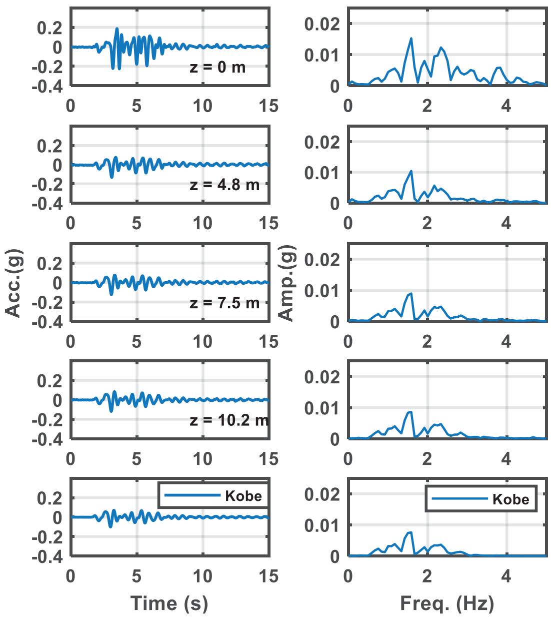

Fig. 6. Acceleration time histories at different elevations of the retaining wall in the saturated test.

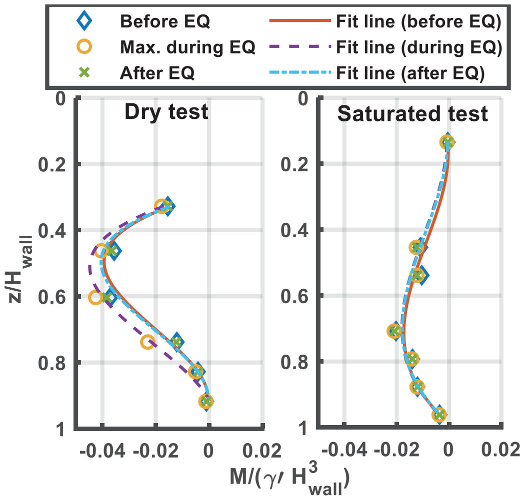

Fig. 7. Bending moment distributions in the retaining wall in the dry and saturated tests.

4 CONCLUSIONS

Two dynamic centrifuge tests were conducted on two structure-soil-wall systems in dry and saturated sand to study the dynamic response of the structure placed behind a retaining wall. The results show that the dynamic response of the structure on the saturated sand was different from that on the dry sand, in terms of the frequency components in the accelerations at the top of the structure. Additionally, the structure was more likely to collapse when the soil beneath was saturated. The distributions of the bending moments were also different in the dry and saturated sand. In dry sand, the peak bending moment is larger and occurs much higher up compared to the saturated sand. This suggests that the bending moments in the wall are relieved due to 'straightening' of the wall in saturated soil, while the dry sand restricts the wall from such 'straightening'.

REFERENCES

Madabhushi, S.P.G., Houghton, N.E. and Haigh, S.K. 2006. A new automatic sand pourer for model preparation at University of Cambridge. Proc. ICPMG, 217-222.

Madabhushi, S.P.G., Haigh, S.K., Houghton, N.E. and Gould, E. 2012. Development of a servo-hydraulic earthquake actuator for the Cambridge Turner beam centrifuge. International Journal of Physical Modelling in Geotechnics, 12(2), 77-88.

Madabhushi, S.P.G. 2017. Centrifuge modelling for civil engineers. CRC Press.

Mitrani, H. 2006. Liquefaction remediation techniques for existing buildings, PhD Thesis, University of Cambridge.

Schofield, A.N., 1980. Cambridge geotechnical centrifuge operations. Geotechnique, 30(3), pp.227-268.

Steedman, R.S., and Madabhushi, S.P.G. 1991. Wave propagation in sand medium. In Proceedings of the 4th international conference on seismic zonation. Earthquake Engineering Research Institute.

Steedman, R.S., and Madabhushi, S.P.G. 1991. Wave propagation in sand medium. In Proceedings of the 4th international conference on seismic zonation. Earthquake Engineering Research Institute